Progress in Oceanography

Vertically resolved zooplankton biomass and size-structure across a continental shelf under the influence of a western boundary current
--Manuscript Draft--

1 **Vertically resolved zooplankton biomass and size-structure across a continental shelf**

2 **under the influence of a western boundary current**

3

4 Hayden T. Schilling[1,2], Jason D. Everett[2,3], Amandine Schaeffer[4,2], Peter Yates[1,2], Mark E.

5 Baird[5], Iain M. Suthers[1,2]

6

7 [1]Sydney Institute of Marine Science, Chowder Bay Road, Mosman, New South Wales,

8 Australia

9 [2]Centre for Marine Science & Innovation, UNSW Australia, Kensington, New South Wales,

10 Australia

11 [3]Centre for Applications in Natural Resource Mathematics (CARM), School of Mathematics

12 and Physics, University of Queensland, Brisbane, QLD, Australia

13 [4]School of Mathematics and Statistics, UNSW Australia, Kensington, New South Wales,

14 Australia

15 [5]Commonwealth Scientific and Industrial Research Organisation, Castray Esplanade, Battery

16 Point, Tasmania, Australia

17 Corresponding author: Hayden T. Schilling (h.schilling@unsw.edu.au)

18

19

20 Main text ≈ 6500 words, 1 Table, 8 Figures

21

Abstract

Continental shelves are the interface between society and the oceans, supporting over 90% of the world's fisheries through highly productive ecosystems. Boundary currents drive oceanographic processes on many continental shelves, yet it is uncertain how boundary currents affect the continental shelf zooplankton community. With an optical plankton counter and CTD mounted on an undulating towed body, we present the first high-resolution vertically resolved profiles of the zooplankton size structure across four transects over a continental shelf. Zooplankton biomass is highest inshore, which declines with increasing distance from shore and with increasing depth in the water column. The front between the warm East Australian Current (EAC) and cooler continental shelf waters also showed increased biomass of zooplankton. Landward of the front is the inner-shelf water, created by EAC uplifting slope waters, resulting in zooplankton ecosystems with smaller geometric mean sizes and steeper size spectrum slopes. South of the EAC separation from the coast, the continental shelf zooplankton was more spatially homogenous but still displayed the same horizontal and vertical patterns in zooplankton. These patterns are consistent with zooplankton distributions on other continental shelves where the inner-shelf has higher biomass of zooplankton with a steeper NBSS-slope compared to offshore. Inner-shelf zooplankton communities support important temperate reef ecosystems and coastal fisheries, through their consistently high biomass.

Key words: Upwelling, Size spectrum, Optical Plankton Counter, Production, East Australian Current, Great Southern Reef

2

Introduction

Continental shelves are the interface between society and the oceans. While accounting for less than 7% of the earth's ocean surface area, continental shelf regions support over 90% of the world's fisheries catch (Pauly *et al.*, 2002). These fisheries are supported by high chlorophyll *a* biomass, often driven by the coastal processes including upwelling, river plumes, boundary currents, and eddies. The high chlorophyll *a* levels often observed on the continental shelf, particularly the inner shelf (Lucas *et al.*, 2011) are a key driver of zooplankton communities which are a key resource for fisheries. In boundary current systems such as the East Australian Current and the Benguela Current, zooplankton can support over 50% of fish biomass on coastal reefs (Truong *et al.*, 2017; Maia *et al.*, 2018), making it a key link between primary production and higher trophic levels.

The transfer of energy between trophic levels is complex but as predation is largely driven by size in the marine environment (Barnes *et al.*, 2010), the size frequency distribution of a community can provide valuable insight. Within a community, the size of all individuals, irrespective of species identity, can be described by the size-frequency which typically yields a histogram that is strongly right-skewed with many small individuals, and a few large individuals (Blanchard *et al.*, 2017; Heneghan *et al.*, 2019). On log-log axes, the negative linear slope of the zooplankton size spectrum (Sprules and Barth, 2015; Edwards *et al.*, 2017), provides insight into energy transfer and community function (Kerr and Dickie, 2001; White *et al.*, 2007). The size spectrum implicitly reflects the outcome of all ecological processes including predation, the growth of individuals through different size classes, and the repopulation of smaller size classes through reproduction (Sprules and Barth, 2015; Andersen *et al.*, 2016; Blanchard *et al.*, 2017). The elevation of the spectrum reflects the environmental effects of nutrients and temperature and can result in differences between

3

69   water masses (Baird *et al.*, 2008). Steeper slopes in the size-spectrum represent inefficient

70   energy transfer between trophic levels which can occur under both oligotrophic conditions

71   as nutrients become scarce and eutrophic conditions as many bloom taxa are relatively

72   large yet unpalatable which increases the chances of mass sinking of ungrazed blooms

73   leading to reduced efficiency of energy transfer (Atkinson *et al.*, 2020).

74   Cross-shelf patterns in zooplankton size spectrum slopes have been examined on

75   several continental shelves. In the southwest Atlantic, the zooplankton community on the

76   continental shelf had higher biomass and a steeper zooplankton size spectrum slope

77   compared to the offshore oceanic stations which were typically more stratified with higher

78   biomass at depth (Marcolin *et al.*, 2013). This is similar to the northeast Atlantic where high

79   zooplankton biomasses and steeper zooplankton size spectrum slopes were found in some

80   but not all inshore regions (Sourisseau and Carlotti, 2006; Irigoien *et al.*, 2009; Vandromme

81   *et al.*, 2014). Fewer studies have examined the vertical patterns of zooplankton on

82   continental shelves and this remains a key knowledge gap. During late summer, in the

83   northwest Atlantic, the vertical zooplankton distribution was strongly influenced by water

84   mass with distinct zooplankton communities separated by a strong thermocline (Turner and

85   Dagg, 1983). In a more homogenous water mass during winter on the Abrolhos Bank in the

86   southwest Atlantic, copepod abundance peaked near the surface (20 – 40 m) and decreased

87   with depth in the water column (Marcolin *et al.*, 2015). The causes of the observed patterns

88   in zooplankton communities on continental shelves remain uncertain with oceanography,

89   particularly boundary currents playing a key role.

90   Boundary currents are important drivers of productivity along continental shelves.

91   Eastern boundary currents directly supply nutrient rich, cool waters from the poles towards

92   the equator which then interact with wind driven upwelling to produce some of the most

4

93   productive fisheries in the world including those located in the Humboldt and California

94   currents (Carr and Kearns, 2003). By contrast, western boundary currents (WBCs) are

95   narrow currents which swiftly move warm oligotrophic water poleward. When WBCs

96   interact with the adjacent continental shelf they induce upwelling of cold nutrient rich water

97   on the inshore edge, generate eddies and form frontal regions (Everett *et al.*, 2012;

98   Schaeffer *et al.*, 2013, 2014; Aguiar *et al.*, 2014). These processes facilitate a nutrient and

99   productivity gradient from the oligotrophic WBC across the continental shelf into the coast.

100   The interaction of the WBC and continental shelf water dominates the pathways by which

101   nutrients and biological materials enter and leave the continental shelf system (Malan *et al.*,

102   2020).

103   Within both eastern and western boundary currents, cross-shelf flows are far smaller

104   in magnitude than along-shelf flows but have a disproportional impact on shelf water

105   properties such as plankton and fish distribution (Brink, 2016). Cross-shelf gradients in

106   chlorophyll *a* (as a proxy for phytoplankton biomass) are commonly observed but are

107   strongly influenced at the smaller-spatial scale by eddies and upwelling (Lucas *et al.*, 2011;

108   Everett *et al.*, 2014). The cross-shelf gradient in chlorophyll *a* may be a key driver of

109   increased zooplankton biomass which is often observed on continental shelves compared to

110   offshore regions, particularly in the northeast (Sourisseau and Carlotti, 2006; Irigoien *et al.*,

111   2009; Vandromme *et al.*, 2014) and southwest Atlantic (Marcolin *et al.*, 2013; Pereira

112   Brandini *et al.*, 2014).

113   The western boundary current of the South Pacific is the East Australian Current

114   which generates eddies (Everett et al 2012) and drives upwelling as it interacts with the

115   continental shelf (Roughan and Middleton, 2002). These oceanographic processes influence

116   nutrient availability and the biomass of chlorophyll *a* (Everett *et al.*, 2014), yet there are no

117   studies investigating the influence of the EAC driven production on higher trophic levels

118   including zooplankton. Here we investigate horizontal and vertical patterns in the

119   zooplankton community using four high-resolution vertically resolved, cross-shelf transects

120   of zooplankton on the eastern continental shelf of Australia to:

121   1) Identify latitudinal differences in zooplankton distribution across the continental

122   shelf in relation to the EAC, and

123   2) Examine the potential drivers of the observed patterns in zooplankton biomass

124   and size-structure, and

125   3) Relate our observations to previous research to propose a general concept of

126   zooplankton size-structure on continental shelves globally.

127

Materials and Methods

Study Region

The East Australian Current (EAC) is the western boundary current of the South Pacific gyre, forming between 10 and 20°S where the South Equatorial Current bifurcates off the Great Barrier Reef and north-eastern Australia (Ridgway and Dunn, 2003). The southward flowing component forms the EAC, flowing at 0.5 – 1.5 m s^{-1} along the continental shelf (Archer *et al.*, 2017) until the majority of the EAC separates from the coast between approximately 30 – 32°S and flows eastward as the EAC eastern extension (Cetina-Heredia *et al.*, 2014; Oke *et al.*, 2019). The remaining portion of the EAC continues to flow south along the coast as part of the EAC southern extension generating a large eddy field (Everett *et al.*, 2012). Along the continental shelf, particularly where the continental shelf narrows, the EAC has significant impact on shelf circulation (Schaeffer and Roughan, 2015). Current driven bottom friction leads to Ekman transport in the bottom boundary layer, moving cooler denser water up the slope, resulting in uplift of isotherms and upwelling (Schaeffer *et al.*, 2014). These intrusion events have been shown to bring nutrient rich water into the euphotic zone, increasing nitrate (Rossi *et al.*, 2014) and chlorophyll *a* concentration (Everett *et al.*, 2014), and controlling vertical phytoplankton abundance and composition (Armbrecht *et al.*, 2014, 2015).

From 2nd – 13th September 2004, a research voyage on the on the RV Southern Surveyor was undertaken from Sydney, Australia (33.82°S, 151.29°E) to Brisbane, Australia (27.36°S, 153.17°E). During this period, the EAC was flowing southward along the coast until approximately 31°S where it separated from the mainland and continued flowing to the

150 east. This separation resulted in the formation of a large warm-core eddy forming off the

151 coast at approximately 33°S, 155°E (Figure 1).

152
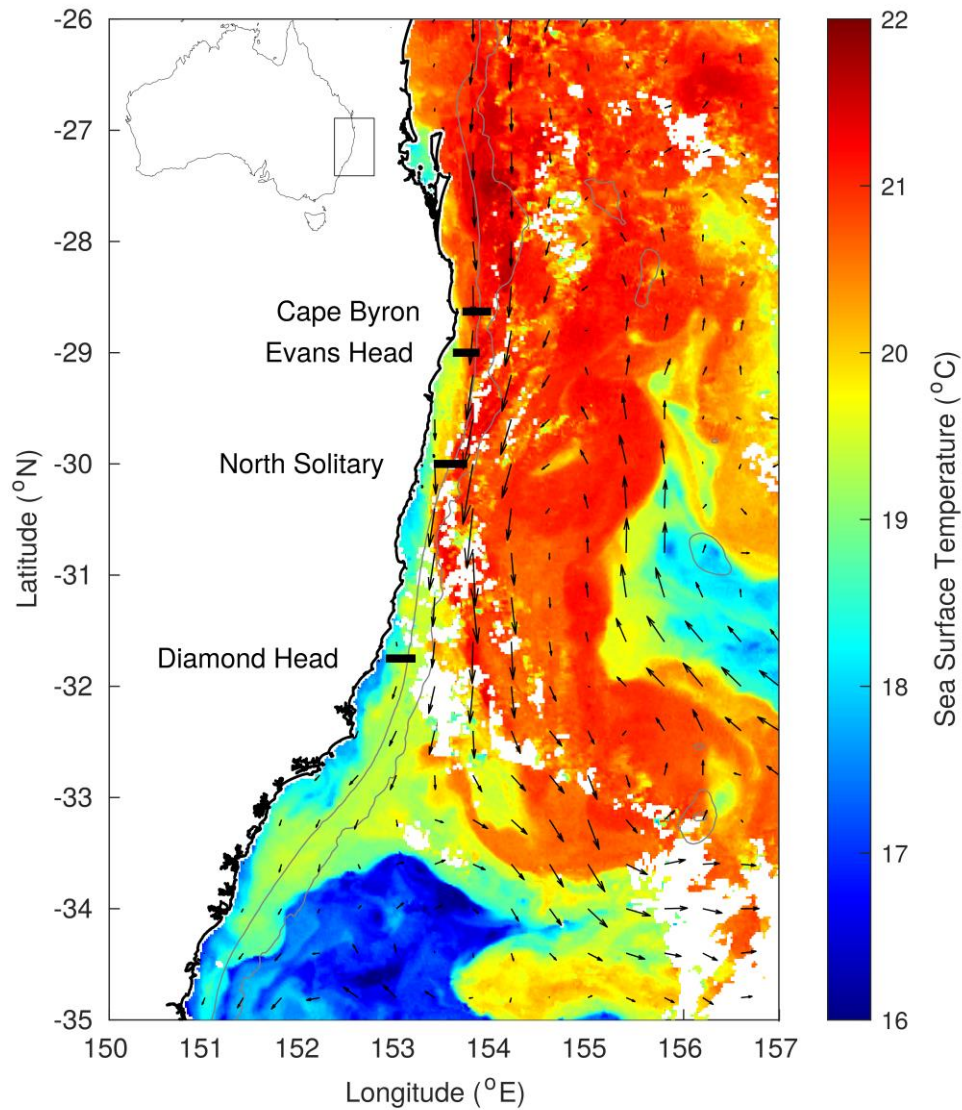
153 **Figure 1** Locations of the four cross shelf sections which were sampled in September 2004.

154 The sea-surface temperature for 6th September 2004 is shown in colour with velocity arrows

155 from satellite altimetry shown with black arrows. Grey isobaths represent 200 and 2000m

156 depths.

157

158   *Sampling*

159   Four transects were sampled roughly perpendicular to the coast over a seven-day period

160   (6th – 12th September; Table 1, Figure 1) using a modified SeaSoar. The SeaSoar was towed

161   from inshore to offshore and undulated between 10 and 120 m depth as used in previous

162   studies (Baird *et al.*, 2008). Mounted on the SeaSoar was a dual CTD system (custom made

163   interface combining a Seabird SBE3 temperature sensor, a Seabird SBE4 conductivity sensor

164   and a Paroscientific 43K-027 pressure sensor) and an Optical Plankton Counter (OPC;

165   Herman 1992) to continuously measure temperature, salinity and the size frequency

166   distribution of particulate matter. An ADCP (Teledyne R. D. Instruments, USA, Model # VM-

167   150) continuously monitored the current velocity profile beneath the vessel. Alongshore

168   and cross-shelf velocity of currents was calculated by rotating the U and V vectors to

169   account for the angle of the coastline at each location (Table 1).

170

171

172 **Table 1** Summary of the four transects undertaken using the SeaSoar with attached optical

173 plankton counter and CTD. Times are local, Australian Eastern Standard Time (GMT +10).

Transect	Coastline Angle (°)	Start Longitude (° E)	Start Latitude (° S)	End Longitude (° E)	End Latitude (° S)	Start Time	End Time
Cape Byron	356	153.704	28.633	153.981	28.633	12/09/2004 08:11	12/09/2004 09:59
Evans Head	13	153.611	28.997	153.858	29.002	11/09/2004 10:55	11/09/2004 12:36
North Solitary	15	153.412	29.998	153.726	29.997	7/09/2004 21:41	8/09/2004 00:05
Diamond Head	19	152.913	31.752	153.191	31.747	6/09/2004 20:00	6/09/2004 21:53

174

Environmental Data

176   To investigate environmental conditions leading up to and during the sampling of

177 transects on the east Australian continental shelf, MODIS-Aqua Level 3 ocean-colour data

178 (chlorophyll-a) were obtained from the Integrated Marine Observing System (IMOS) Data

179 Portal (http://imos.aodn.org.au/imos/) at 1 km resolution. Chlorophyll-a was derived using

180 the OC3 algorithm. Sea surface temperature was obtained from L3S AVHRR daily night

181 product from the same portal, displayed as a map for the region (resolution of 0.02°).

182 Surface geostrophic currents were derived from gridded sea level gradients from satellite

183 altimetry, also taking into account sea level gauges to improve the estimate in coastal area

184 (resolution of 0.2°). To quantify lead-up conditions to our sampling, MODIS chlorophyll-a

10

185   data were retrieved for 5×5 pixels (~25 km^2) surrounding the western and eastern edges of

186   each transect, for the month prior to the day of sampling.

187   To investigate the seasonal variation of EAC strength in the region of our transects,

188   10 years (2004 – 2013) of surface geostrophic currents from satellite altimetry were

189   obtained from the IMOS Data Portal (http://imos.aodn.org.au/imos/) for each of our

190   transects. Alongshore and cross-shelf velocity of currents was calculated by rotating the U

191   and V vectors to account for the angle of the coastline at each location (Table 1). The

192   monthly mean (and standard deviation) alongshore velocity was calculated for the 10-year

193   period by averaging the daily velocities. We assumed that faster alongshore velocity would

194   be due to increased influence of the EAC which is known to seasonally widen, extending its

195   influence over the continental shelf (Archer *et al.*, 2017).

196   The potential influence of wind driven circulation was investigated from wind data

197   from Coffs Harbour meteorological station from the Bureau of Meteorology (30.311°S,

198   153.118°E) located close to shore at 5 m height. The hourly wind stress was calculated

199   following Wood *et al*. (2016). Bathymetric data was sourced from GEBCO (GEBCO

200   Bathymetric Compilation Group, 2019).

201

Zooplankton Size Structure

203   The OPC was a Focal Technologies Corporation Model OPC-2T with a sampling

204   aperture of 2 x 10 cm (Herman, 1992). The OPC records equivalent spherical diameters

205   (ESD) of particles that pass through the instrument in 0.5 s intervals (e.g. Suthers *et al.*,

206   2006; Baird *et al.*, 2008). The particle sizes were recorded digitally using 4096 size bins,

207   corresponding within the operating range of the instrument to bins with a width varying

208   between 5 and 15 µm. The particles used in the following analysis were restricted to those

209   above 250 µm ESD to account for the lower detection limit of the OPC (Suthers *et al.*, 2006).

210   As the region of our study had low chlorophyll-a concentration and turbidity during our

211   study we are confident in assuming there was a low amount of sediment that would not

212   change the results of our assumption that all particles recorded are part of the planktonic

213   ecosystem (Espinasse *et al.*, 2018). As we are most interested in quantifying the overall size-

214   structure trend by looking at general trends in particle size and abundance, hereafter for

215   simplicity, we refer to the OPC counts as zooplankton, but acknowledge that a proportion of

216   the particles will be marine snow, moribund carcasses or appendages, all of which are an

217   important part of the planktonic food web (Alldredge and Silver, 1988; Tsukamoto and

218   Miller, 2020).

219   The volume of flow through the sample region was based on distance measured over

220   a 6 s interval. It has been previously shown that a 6 s interval provides optimal vertical and

221   horizontal resolutions (≈ 6 m vertically) of the size distribution in the Tasman Sea region,

222   near the current study area (Baird *et al.*, 2008). To quantify the zooplankton community,

223   several metrics were calculated for each interval of our transects (Krupica *et al.*, 2012).

224   These included total biomass (mg m^{-3}), geometric mean size (GSM; µm ESD) and

225   zooplankton size spectrum slope which we calculated as the shape parameter *c* of the

226   Pareto distribution of the particles (equivalent to the traditional NBSS slope). The OPC

227   records the time and size of each particle detected, allowing the Pareto distribution to be

228   calculated without further binning of the raw digital signal that is necessary for the NBSS.

229   The correlation between the more common NBSS Slope and shape parameter *c* of the

230   Pareto distribution was also tested to confirm the relationship. The Pareto distribution has

231 been previously used in this region to spatially resolve the size distribution of particles

232 (Suthers *et al.*, 2006; Baird *et al.*, 2008).

233   The Pareto distribution has a probability density function (*pdf*) defined as:

234
$$pdf(s) = ck^c s^{-(c+1)}$$

235   where *s* is the size of the particle, and *c* and *k* are the distribution's shape and scale

236 parameters, respectively (Vidondo *et al.*, 1997). ESD values (μm) were converted to biomass

237 (mg m^{-3}) as per Wallis et al. (2016), assuming the volume of a sphere and the density of

238 water ($\rho=10^9$ mg m^{-3}) using:

239
$$Biomass\ (mg\ m^{-3}) = \frac{4}{3}\pi \left(\frac{ESD}{2}\right)^3 \rho$$

240 Zooplankton data from the OPC were interpolated to create 2D visualisations of the profiles

241 across the continental shelf using the 'akima' R package to interpolate a regular grid of

242 points via bivariate interpolation (Akima and Gebhardt, 2020), then applying contours

243 within the 'ggplot' package (Wickham 2011).

244

A global context

246 To place our east Australian transects in a global context and identify general trends in

247 zooplankton communities on continental shelves, we examined 18 previous studies which

248 investigated spatial changes in zooplankton communities over continental shelf regions.

249 Where possible from each study we extracted values for total zooplankton biomass,

250 abundance and the zooplankton size spectrum slope from the most inshore and furthest

251 offshore sites (Table S1). From each study we extracted a maximum of one inshore and one

13

252 offshore value, averaged across the study as well as corresponding bathymetry values,

253 except for two studies from the Bay of Biscay (Irigoien *et al.*, 2009; Vandromme *et al.*, 2014),

254 where the east and south regions had very different zooplankton communities so there

255 were kept as distinct regions. If there were multiple years or seasons within a study, an

256 average was taken. As many studies only provided binned values or plots, data were

257 estimated from plots using a colour sampling tool and binned data were assigned values

258 equal to the mid-point of the bin (Table S1). As the studies reported a range of units, to

259 make studies comparable in terms of inshore to offshore trends we present the ratio of

260 inshore to offshore values.

Results

Regional Oceanography

263   The three northern most transects (north of 30°S) all crossed from cool inshore

264   waters into warm (>21 °C) EAC water but the southern transect (Diamond Head 31.75°S)

265   was located south of where the EAC begins to separate from the shelf ("the separation

266   zone"), causing cooler (<19.5 °C) waters (Figure 1). All transects showed low chlorophyll

267   levels (<1.4 mg m^{-3}; Figure S1) which was representative of the previous month of low

268   chlorophyll-a at these locations (Figure S2). Most transects were negligibly influenced by the

269   effects of wind in the 3 days prior to the transects (Figure S3), with most of the wind coming

270   from a southerly direction. The exception was the North Solitary (30°S) transect which was

271   subject to some wind driven upwelling prior to our sampling (Figure S3).

272

Cape Byron (28.6°S)

274   The northernmost transect at Cape Byron (28.6°S) was dominated by the EAC which

275   had a strong alongshore flow (1.50 m s^{-1}) centred over the 200 m isobath (27.6 km

276   offshore). Most of the continental shelf was flooded by warm EAC water (Figure 2). The EAC

277   showed slight onshore movement which increased offshore and with depth, peaking

278   between 100 and 200 m depth (up to 0.26 m s^{-1}, Figure S4). The strong EAC flow resulted in

279   strong current-driven uplift of the isotherms inshore of the EAC with the 21 °C isotherm

280   rising to the surface from 70 m depth over 5 km and the 20 °C isotherm rising to the surface

281   from 100 m depth over 15 km.

282   A decline in zooplankton biomass was observed from both inshore to offshore and

283   from the surface to depth with the highest biomass (~750 mg m^{-3}; Figures 3, S5, S6)

15

284   observed at the surface ~20 km from the coastline, just inshore of the 21 °C isotherm

285   (Figure 3a). This 21 °C isotherm appears to be a strong delineator of both zooplankton

286   biomass and the size distribution. The EAC waters, warmer than 21 °C and > 1.2 m s^{-1}

287   southward velocity, were characterised by low zooplankton biomass with a GMS of ≈450 μm

288   ESD (Figure 4) with steep zooplankton size spectrum slopes between -1 and -1.3 (Figure 5).

289   The cooler water immediately inshore of the 21 °C isotherm had high zooplankton biomass,

290   shallower zooplankton size spectrum slope (-0.9; Figure 5) with larger particles (GMS 500

291   μm ESD; Figure 4)). Further inshore again (15 -17 km from the coastline), in water < 20 °C,

292   biomass remained high (Figure 3), but the particles were smaller (GMS ≈430 μm ESD; Figure

293   4), resulting in a steeper zooplankton size spectrum slope (≈-1.25; Figure 5).
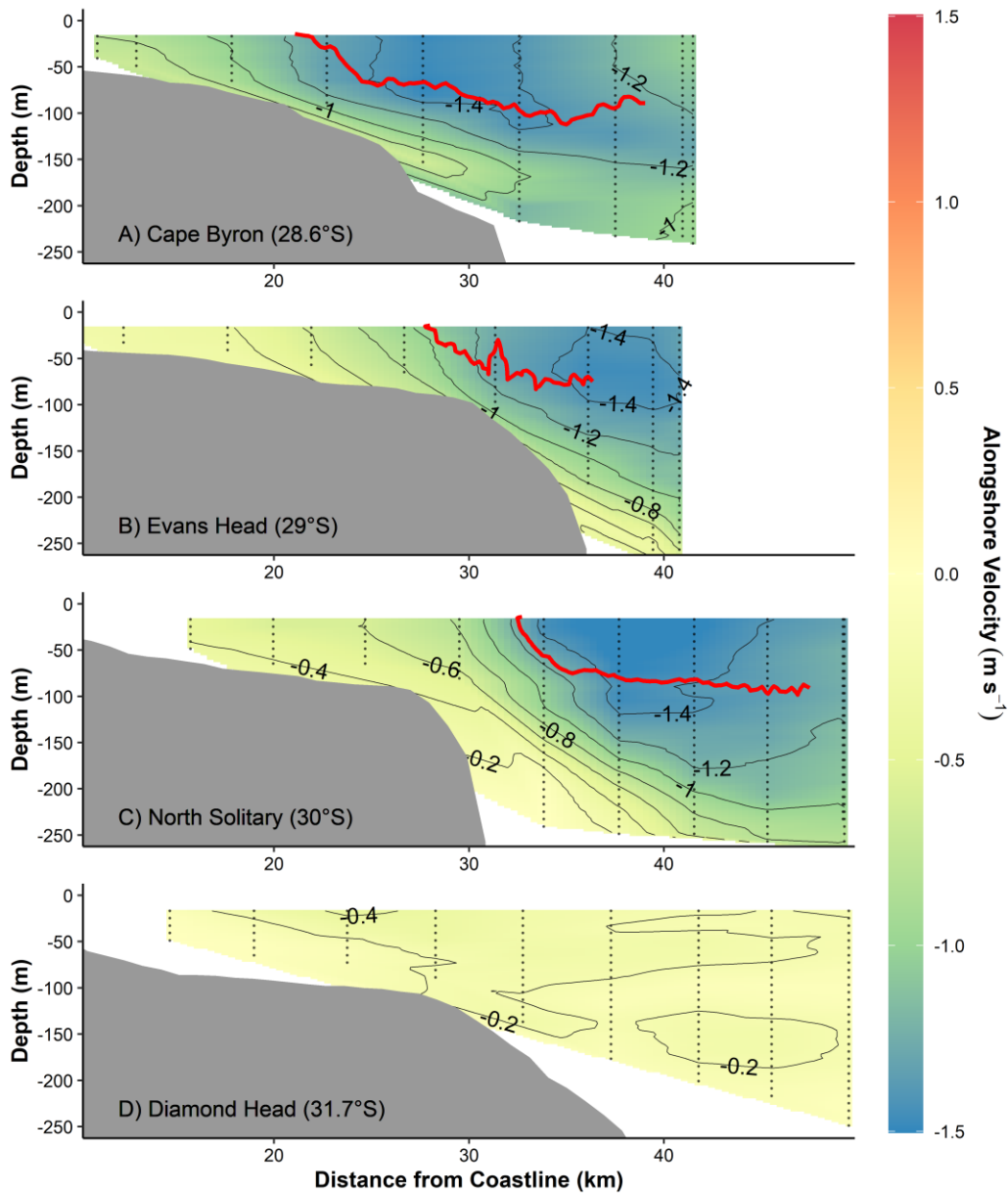
Figure 2 Alongshore velocity across the four cross shelf transects (Figure 1), from the

vessel's Acoustic Doppler Current Profiler. Grey lines join areas of equal velocity. The red

line shows the 21°C isotherm. Note the cooler water where there was no 21°C isotherm for

Diamond Head.

294

295

296

297

298

300
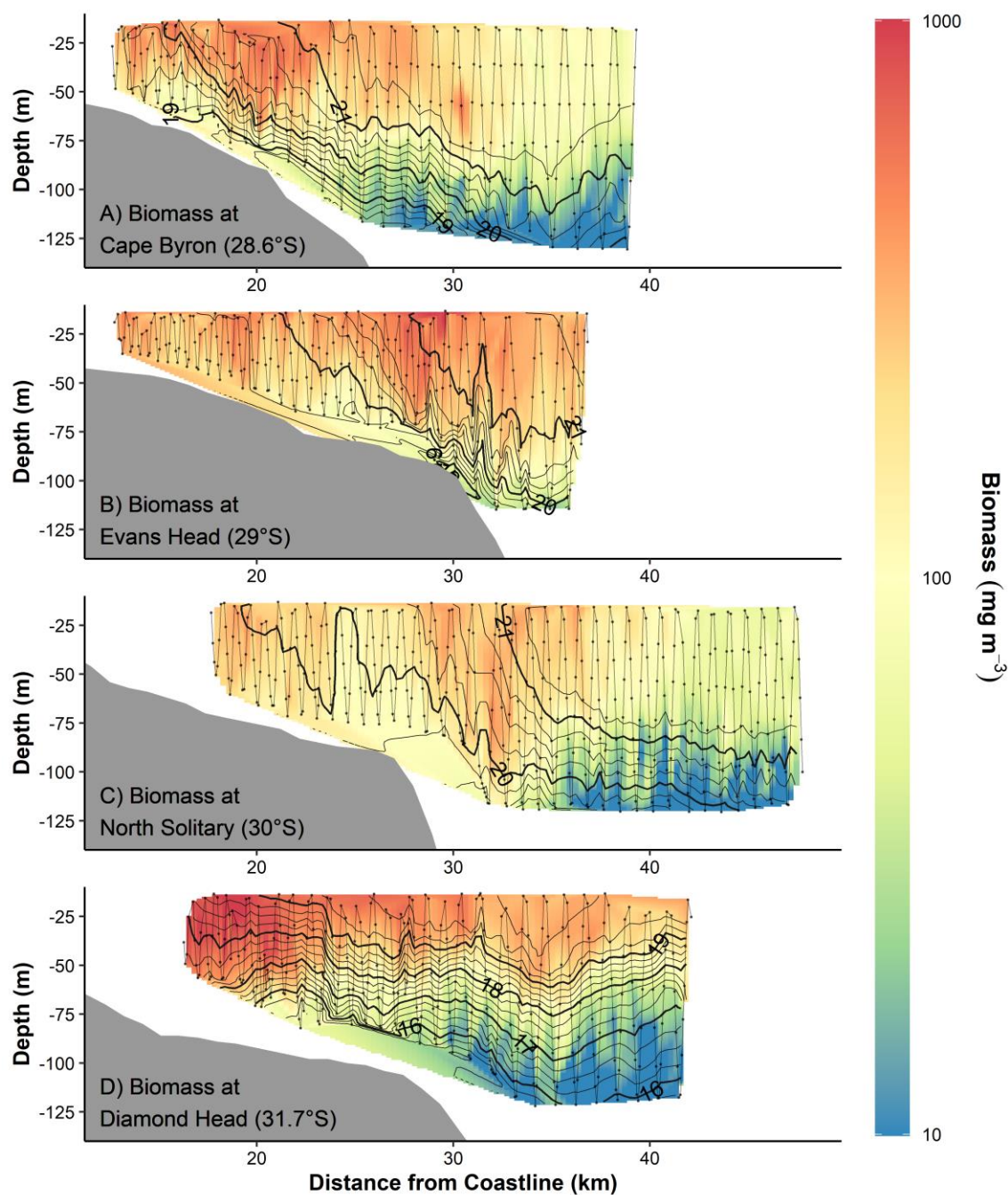
Figure 3 Zooplankton biomass (mg m^{-3}) distributions from the four cross shelf transects

302 (Figure 1). Transects were conducted from inshore to offshore with an undulating towed

303 body with the path shown by the grey line with midpoints of each sample shown as dots.

304 Temperature (°C) isotherms are shown in black. Note the log transformed colour scale.
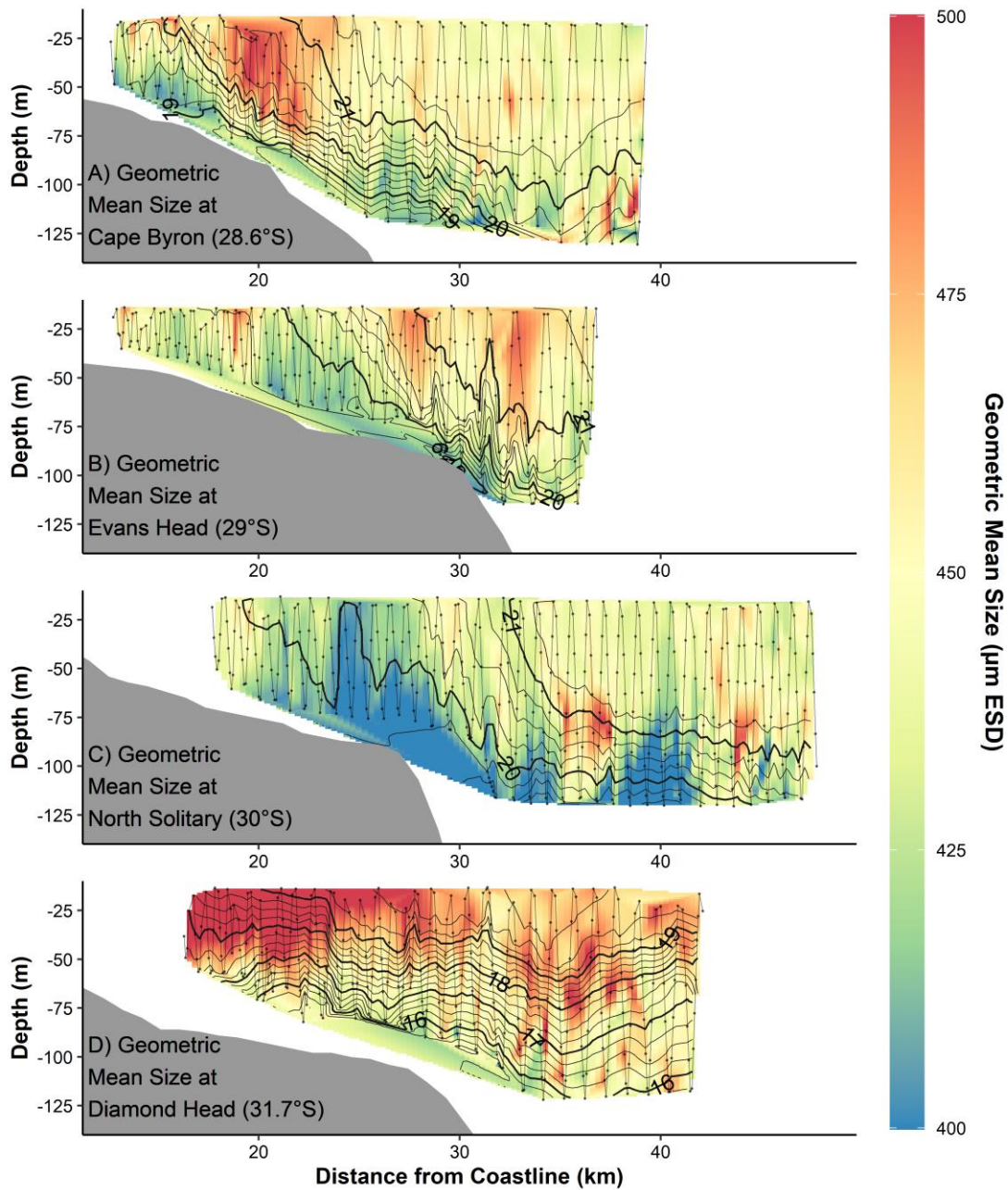
Figure 4 Geometric Mean Size (μm equivalent spherical diameter) of zooplankton from the

four cross shelf transects (Figure 1). Transects were conducted from inshore to offshore

with an undulating towed body with the path shown by the grey line with midpoints of each

sample shown as dots. Temperature (° C) isotherms are shown in black.
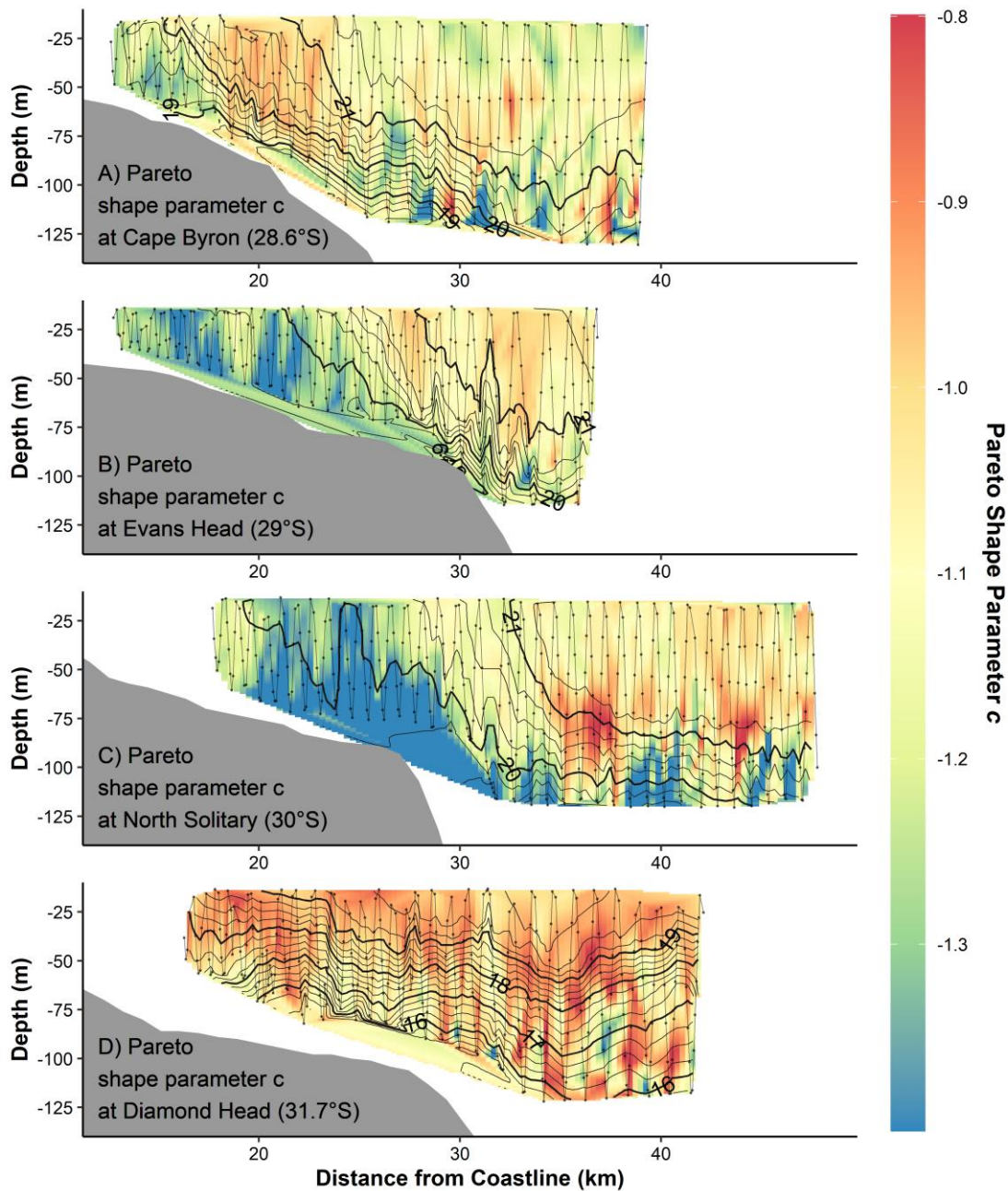
Figure 5 Interpolations of the shape parameter *c* from the Pareto distribution of

zooplankton size from the four cross shelf transects (Figure 1). This is a robust estimate of

the normalised biomass size spectrum slope (shown in Figure S7). Transects were conducted

from inshore to offshore with an undulating towed body with the path shown by the grey

line with midpoints of each sample shown as dots. Temperature (° C) isotherms are shown

in black.

Evans Head (29°S)

318

319   The transect slightly further south at Evans Head (29°S) did not go as far offshore as

320   the other transects but was still largely influenced by the EAC which had a strong along-

321   shore flow (1.47 m s^{-1}) centred 36.1 km from the coast, near the edge of the continental

322   shelf (220 m seabed depth; Figure 2). The EAC showed offshore movement (0.27 m s^{-1})

323   which increased with distance offshore (Figure S4). There was strong current driven uplift of

324   the isotherms inshore of the EAC with the 21 °C isotherm rising to the surface from 70 m

325   depth over 6 km and the 20 °C isotherm rising to the surface from 100 m depth over 15 km

326   similar to the northern Cape Byron site (28.6° S).

327   The zooplankton community was related to the water masses along the transect,

328   especially in relation to water temperature. Around the front between the continental shelf

329   water (< 21 °C) and the warm (> 21 °C) EAC water the zooplankton community showed a

330   similar GMS of ≈450 μm ESD to that observed at the northern Cape Byron transect but had a

331   higher biomass and shallower pareto distribution shape parameter c (≈-1; Figures 3, 4 & 5).

332   In the cool inshore waters < 20°C, there remained high zooplankton biomass (Figure 3), but

333   the community had shifted towards smaller particles which resulted in a steeper c (< -1.3;

334   Figures 4 & 5).

335

North Solitary (30°S)

336

337   The transect at North Solitary (30°S) showed the strongest evidence of current

338   driven uplift of any of the transects with the 21 °C isotherm rising to the surface from 70 m

339   depth over 3 km and the 20 °C isotherm rising to the surface from 100 m depth over 10 km

340   (Figure 3). The offshore portion of the transect continued to be dominated by the EAC which

341   had a strong alongshore flow (1.59 m s^{-1}) centred 37.7 km offshore (310 m bathymetry;

342 Figure 2). The EAC had slight onshore movement, in offshore waters 100-150m below the

343 surface (0.15 m s^{-1}; Figure S4).

344 Like the northern transects, the biomass of the zooplankton community generally

345 decreased with distance offshore and with depth (Figures 3, S5 & S6). The EAC and further

346 offshore, contained low zooplankton biomass with a shallow pareto distribution shape

347 parameter c (-0.9) and GMS of ~450 µm (Figures 3, 4 & 5). The 20 °C isotherm appeared a

348 strong boundary for zooplankton communities with zooplankton in water < 20 °C having

349 relatively low biomass and a much smaller GMS (~400µm ESD) resulting in a steeper c (< -

350 1.3). This was particularly evident where the 20°C isotherm reach the surface ~24 km from

351 the coastline, bringing with it a highly productive zooplankton community (Figures 4 & 5).

352

Diamond Head (31.75°S)

354 The most southern transect located at Diamond Head (31.75°S) was not influenced by the

355 EAC which had separated from the coast to the north and was characterised by a more

356 homogeneous water mass. Here, the alongshore velocities were low (< 0.43 m s^{-1}, Figure 2)

357 with low onshore movement of water (0.11 m s^{-1}) in the surface waters and offshore

358 movement (0.27 m s^{-1}) in the deeper waters (Figure S4). There was minor uplift of the

359 temperature isotherms with all isotherms rising approximately 20 – 40 m as they came onto

360 the continental shelf. This uplift is likely caused by the separation of the EAC from the coast

361 to the north, generating uplift through the creation of eddies near Diamond Head rather

362 than current driven uplift observed at the northern EAC influenced sites (Roughan and

363 Middleton, 2002; Schaeffer and Roughan, 2015).

364 ~~The zooplankton community was not clearly related to water masses reflecting the~~

365 ~~more homogenous water mass here.~~ Inshore, the zooplankton community was charactered

366 by larger individuals (GMS ~500 μm ESD; Figure 4) and had higher overall biomass which

367 declined steadily with distance offshore and with depth (Figures 3, S5 & S6). The pareto

368 distribution shape parameter *c* of the community was shallow over the whole transect (≈-

369 0.9; Figure 5).

370

371 *Synthesis* and *Seasonal Context of the EAC*

372 Satellite altimetry showed throughout the year alongshore velocity varies at our

373 transects by approximately 0.25 m s^{-1} with the more northern sites having the fastest overall

374 flow (Figure 6). The velocity at all sites slows in winter between April and August increasing

375 in Spring (when our observations were taken) and Summer.

376 Both the EAC-influenced transects (three northern ones) and the transect in the

377 separation zone (Diamond Head) showed that generally higher zooplankton biomasses were

378 observed in continental shelf waters with declines offshore and with depth (Figures S5 &

379 S6). Peaks in biomass were also observed at the front between the continental shelf waters

380 and EAC waters (21 °C isotherm; Figure 3). The transect at Evans Head did not show a

381 noticeable decline in biomass with distance from the coast but this transect did not extend

382 past the edge of the continental shelf where the declines were seen in the other 3 transects.

383 Three patterns in GMS were evident in our 4 transects. Cape Byron and Evans Head

384 showed evidence of larger GMS around the front between the warm EAC and cooler inner

385 shelf water (around the 21 °C isotherm; Figure 4). North Solitary showed evidence of uplift

386 with the small GMS community from deep uplifted to the surface. Diamond Head was very

387 different with a more homogenous distribution of GMS although there was a trend of larger

388 zooplankton inshore. The size structure of all sites was related to the GMS with steeper

389 zooplankton size spectrum slopes in areas with smaller zooplankton (Figures 4 & 5). The

23

390 Pareto *c* shape parameter was highly correlated with the NBSS Slope but provided better

391 fewer gaps (due to low numbers of particles) over the transects ($r = 0.934$, $t_{535} = 60.362$, $p <$

392 0.001, Figure S7).

393
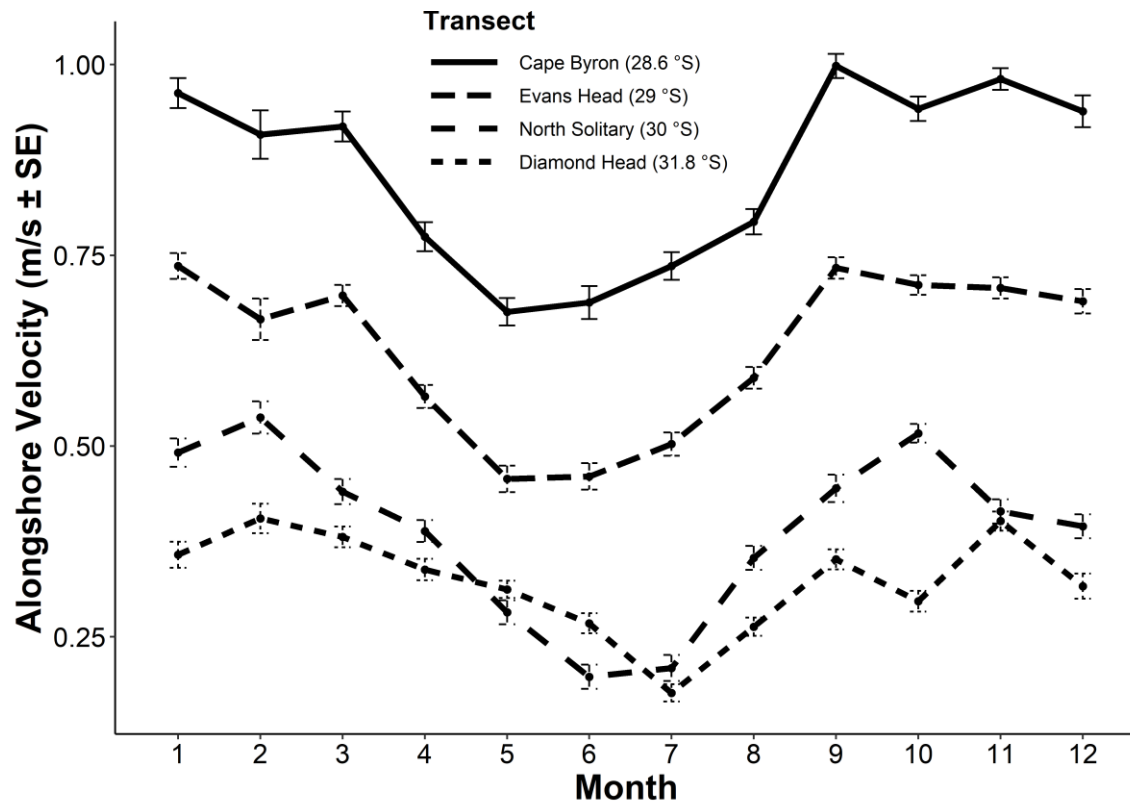
394 **Figure 6** Seasonal changes in mean alongshore surface velocity at the Cape Byron (28.6°S),

395 Evans Head (29°S), North Solitary Island (30°S) and Diamond Head (31.8°S) based upon 10

396 years of satellite altimetry data (2004 – 2013). Velocity data was downloaded for the

397 eastern edge of each transect (Table 1) from the IMOS Data Portal

398 (http://imos.aodn.org.au/imos/). The EAC separates from the coastline between

399 approximately 28°S and 32°S (Cetina-Heredia *et al.*, 2014).

400

401 *Global Synthesis*

402 19 studies quantified the cross-shelf changes in zooplankton (including this study), revealing

403 a broad consensus (Figure 7; Table S1), even though many studies were not influenced by a

404   western boundary current. Seven studies (including ours) reported abundance values for

405   inshore and offshore and all found that abundance was higher in inshore regions compared

406   to offshore regions. Six of these studies showed inshore areas abundance of 2.3 – 4.2 times

407   higher than offshore values with one study from the eastern Bay of Biscay region finding a

408   22-fold difference (Sourisseau and Carlotti, 2006). For biomass, six of seven studies showed

409   1.5 – 4.1-fold greater biomass inshore compared with offshore (Figure 7; Table S1). The sixth

410   study from the Western Mediterranean showed 20-fold higher biomass offshore compared

411   to inshore values (Sabatès *et al.*, 1989).

412   In terms of size structure, 11 studies reported both inshore and offshore values with

413   nine finding steeper zooplankton size spectrum slopes in inshore areas compared with

414   offshore areas (Figure 7, Table S1). The southern Bay of Biscay and North Iberian Shelf

415   studies were unusual in having a shallower inshore zooplankton size spectrum slope

416   compared to the offshore areas (Nogueira *et al.*, 2004; Vandromme *et al.*, 2014).

417
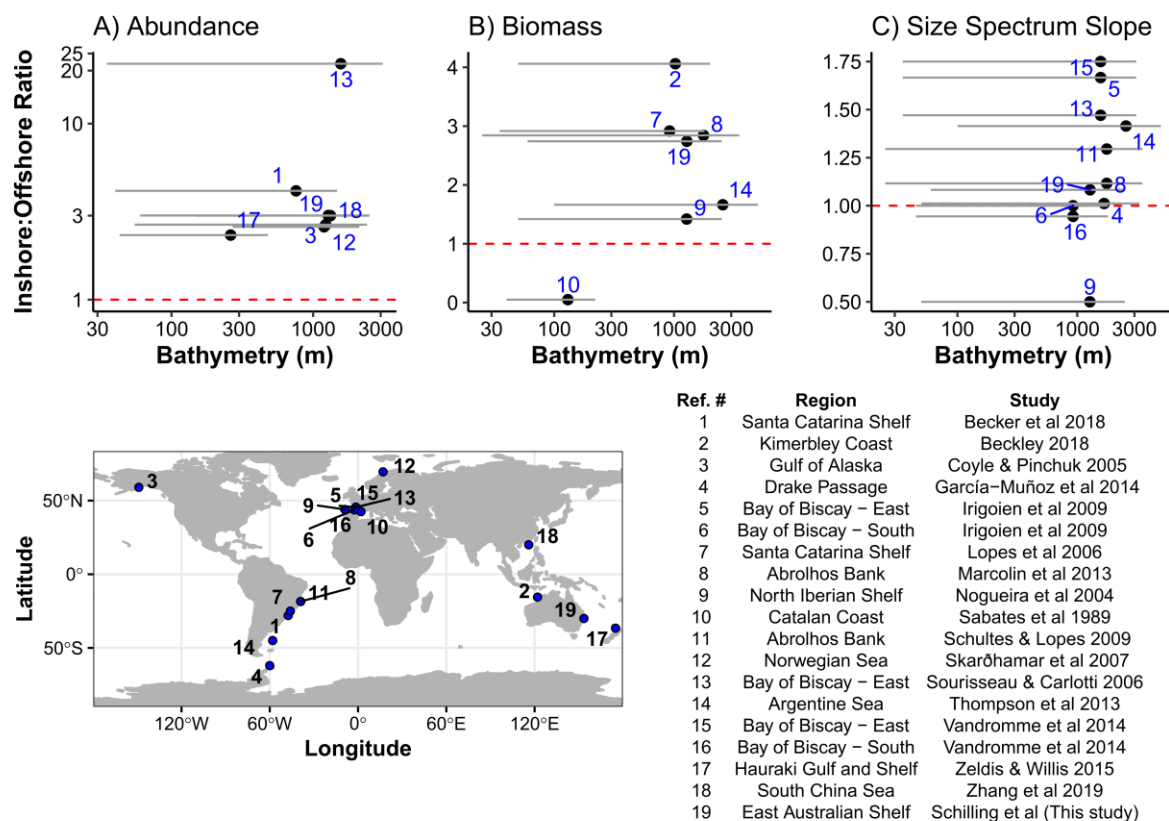
418   **Figure 7** Summary of 18 previous studies investigating cross shelf patterns of zooplankton

419   (#19 is the current study). The y-axis shows the ratio of the inshore to offshore reported

420   values for zooplankton A) Abundance, B) Biomass, and C) the Size Spectrum Slopes. A ratio

421   greater than 1 (red dashed line) means that the inshore region had a larger

422   abundance/biomass or steeper size spectrum. Each numbered dot represents a study

423   except for the studies in the Bay of Biscay which identified east and south as distinct region

424   so they remain independent (Table S1; Irigoien *et al.*, 2009; Vandromme *et al.*, 2014). The x-

425   axis represents the bathymetry range from each study with the dot on the mean value for

426   that study. Note the differing y-axes and $\log_{10}$ x-axis on a), and that not all studies are in

427   western boundary current influenced locations.

428

429

Discussion

430

431   The size-spectrum of zooplankton provides important information about the transfer

432   of energy from phytoplankton to fish, from which we can learn more about the fisheries

433   supported by our continental shelves. We found consistent declines from inshore to

434   offshore in zooplankton biomass and altered size-structure horizontally and vertically across

435   the narrow continental shelf off eastern Australia. These trends in the ~~zooplankton~~

436   ~~community~~ are consistent with the patterns in zooplankton size-structure across other

437   continental shelves (Figure 8) and are an outcome of cross-shelf flows and sporadic

438   upwelling processes driven by ocean currents and coastal winds (Roughan and Middleton,

439   2002; Everett *et al.*, 2014; Malan *et al.*, 2020).

440   Zooplankton biomass and mean size was generally constrained by the horizonal and

441   vertical structure of the water column over the continental shelf. Peaks in zooplankton

442   biomass coincided with the front between the continental shelf water and oligotrophic EAC,

443   where the interaction of water masses often creates strong instabilities and vertical

444   velocities producing a highly productive environment (Nakata *et al.*, 2000; Baird *et al.*,

445   2008). Distinct from the warmer offshore EAC, the cooler shelf water revealed a

446   ~~zooplankton community~~ with higher ~~biomass,~~ smaller geometric mean size and steeper size

447   spectrum slope (Figure 8). These observations are consistent with higher chlorophyll *a* on

448   the continental shelf (Everett *et al.*, 2014) and are likely driven by uplift of the cooler water

449   due to the EAC interacting with the sloping topography (Schaeffer and Roughan, 2015). As

450   zooplankton are the basis of many coastal food webs, this consistent supply of nutrients is

451   an important factor in the distribution and abundance of planktivorous fish and the higher

452   trophic level fisheries found on continental shelves (Pauly *et al.*, 2002; Truong *et al.*, 2017;

453   Holland *et al.*, 2020).

27
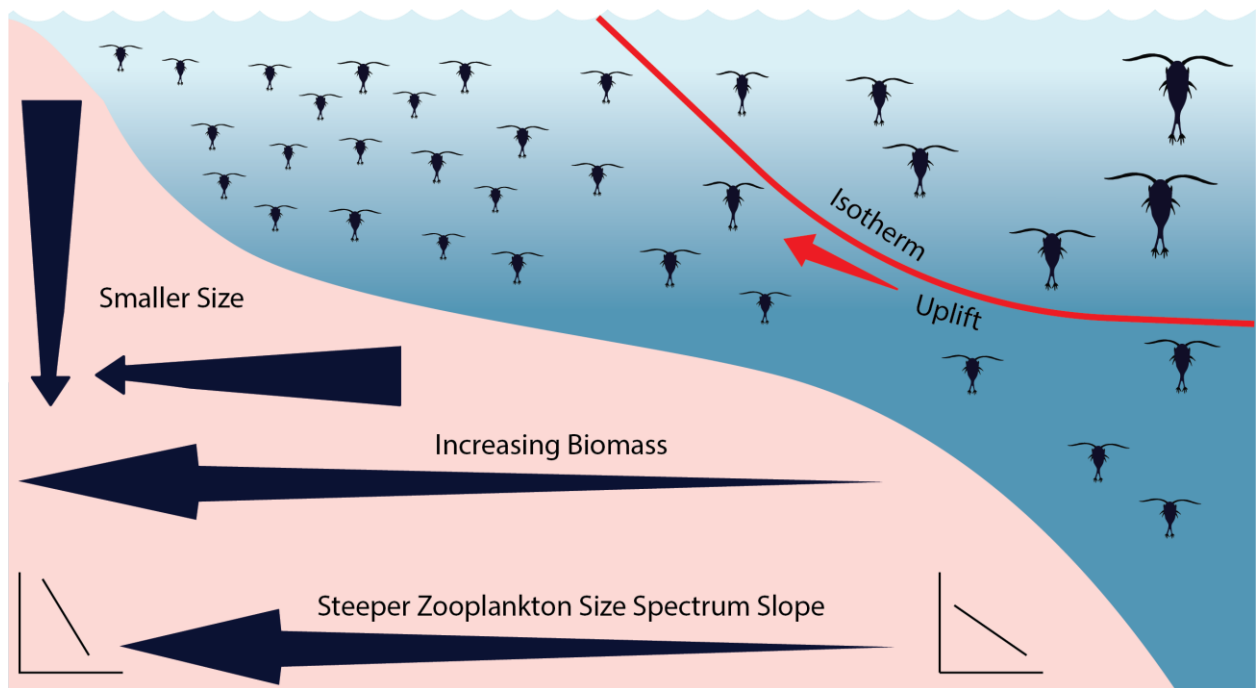
Figure 8 Conceptual diagram of the zooplankton community and how it changes over a continental shelf and with depth. Note all zooplankton are represented by copepods in this diagram.

Effects of the EAC on zooplankton

The separation of the EAC from the Australian coast, where it often bifurcates towards the east, forms a front between the northern oligotrophic waters, and the southern eutrophic Tasman Sea waters (Oke *et al.*, 2019). Offshore, this can separate distinct zooplankton communities (Baird *et al.*, 2008) and with impacts on abundance and diet of fish (Hobday and Hartmann, 2006; Revill *et al.*, 2009). On the continental shelf, the influence of the EAC separation on the distribution of zooplankton and fish is less well known. Our results suggest that along the three northern transects strongly influenced by the EAC, the continental shelf waters are influenced by uplift of deep nutrient-rich water (Roughan and Middleton, 2002), which drives the higher biomass of phytoplankton (Everett *et al.*, 2014) and zooplankton. Closer inshore, the effects of predation pressure from fish in the littoral

470   zone, particularly on temperate reefs, may remove larger plankton (Truong *et al.*, 2017;

471   Holland *et al.*, 2020). Therefore a steeper zooplankton size spectrum slope could arise not

472   only from increased production of smaller zooplankton (Guiet *et al.*, 2016), but also by

473   predation on larger zooplankton prey by planktivorous fish (Moore and Suthers, 2006).

474   In contrast to the northern transects, the southern transect (Diamond Head; 31.75°S)

475   was south of the EAC separation zone and dominated by Tasman Sea water resulting in

476   larger particles and a shallower zooplankton size spectrum slope. The same pattern of

477   decreasing biomass offshore, and with depth in the water column occurred. In general, the

478   Tasman Sea has an elevated nutrient concentration and higher zooplankton biomass

479   compared to the oligotrophic EAC waters (Baird *et al.*, 2008). At our southern site there are

480   two possibilities for this cross shelf gradient. Firstly, as there was minimal EAC influence at

481   the southern site it is possible that the zooplankton are being retained on the continental

482   shelf in this location due to weak flow in the lee of the EAC separation (Everett *et al.*, 2014;

483   Schaeffer and Roughan, 2015). Secondly, this region has been shown to have high

484   chlorophyll *a* production due to both wind driven and current driven upwelling with wind

485   driven upwelling reliably generating increases in chlorophyll *a* (Everett *et al.*, 2014). This

486   production may then flow through into the zooplankton community.

487   Previous research on the biophysical properties of oceanographic fronts in this

488   region demonstrated an order of magnitude increase in the biomass of zooplankton in

489   frontal regions (Baird *et al.*, 2008), ~~similar to our observations of a increase in both~~

490   ~~zooplankton biomass and a steeper size spectrum slope at the front between the~~

491   ~~continental shelf water and warm EAC water.~~ This increase in productivity around fronts

492   may be a driver of previously observed relationships between fish abundance and frontal

493   features (Fiedler and Bernard, 1987; Reese *et al.*, 2011).

494   Where there are interactions of currents (such as at fronts) or other upwelling

495 promoting mechanisms, such as boundary currents, there is consistently higher zooplankton

496 biomass and a steeper zooplankton size spectrum inshore compared to offshore (Figure 7,

497 8). Due to the increased production, there is typically high production of small zooplankton

498 with increased abundance and biomass transferred to the larger size classes and higher

499 trophic levels.

500   While this study provides the first high-resolution depth-resolved cross shelf

501 transects, we did not sample in areas where the bathymetry was less than 50 m, meaning

502 that the inshore water masses which may be more heavily influenced by terrestrial inputs,

503 waves, wind-driven vertical mixing, and interactions with the coastline were not sampled.

504

505 *Comparison to other studies*

506   Our study showed a consistent decline in biomass horizontally (increasing distance

507 from shore) and vertically (increasing depth in the water column) with the largest biomasses

508 observed in the surface inner shelf waters. This was similar to almost all other comparable

509 studies with the exception being the western Mediterranean which is not located in a

510 boundary current system but included in our continental shelf comparison for completeness

511 (Sabatès *et al.*, 1989). In the northeast Atlantic, the declining pattern of biomass across the

512 shelf was attributed to coastal nutrient inputs and long residence times of water masses

513 over the shelf break (Sourisseau and Carlotti, 2006; Irigoien *et al.*, 2009; Vandromme *et al.*,

514 2014). However, in the Brazilian Bight (southwest Atlantic), the increase in inshore

515 zooplankton biomass was attributed to bottom intrusions of cooler nutrient rich South

516 Atlantic Central Water (Pereira Brandini *et al.*, 2014). To the south, similar results were

517 observed on the Abrolhos Bank where higher zooplankton biomass was observed on the

518 continental shelf due to the Brazilian Current interacting with the sea-floor, generating uplift

519 and eddies which increased mixing over the continental shelf (Marcolin *et al.*, 2013).

520 In regions such as the southwest Pacific where our study was conducted, there are

521 relatively small terrestrial influences compared to other sources of nutrients such as

522 upwelling (Apte *et al.*, 1998; Dai and Trenberth, 2002; Pritchard *et al.*, 2003; Suthers *et al.*,

523 2011), and oceanographic drivers are important. Similar to the Brazilian Current and the

524 Abrolhos bank, in the southwest Pacific the EAC interacts with the topography which in turn

525 generates uplift of cooler water onto the continental shelf (Roughan and Middleton, 2002).

526 Steeper zooplankton size spectrum slopes in inshore regions is another feature of

527 zooplankton communities which are consistently observed. In some regions the areas of

528 steepest slopes have been linked to estuarine-derived nutrients (Moore and Suthers, 2006;

529 Irigoien *et al.*, 2009), which are exploited by nearshore planktonic communities while steep

530 slopes occurring further offshore are more temporally consistent and potentially due to

531 local circulation patterns and retention (Vandromme *et al.*, 2014). Within the cross-shelf

532 patterns of zooplankton, biomass and mean size also tend to decline with depth in the

533 water column, possibly as a response to light availability (Aarflot *et al.*, 2019).

534 There are exceptions to the general trends in biomass, abundance and size spectrum

535 slope. For example, Nogueira et al. (2004) showed a shallow inshore slope compared to

536 offshore, which was attributed to nearby continental inputs increasing the proportion of

537 large zooplankton possibly due to a eutrophic environment (Atkinson *et al.*, 2020). Some

538 studies also show these onshore-offshore gradients are highly variable as observed in the

539 East China Sea where onshore-offshore gradients in different years showed no consistency,

540 but insufficient data was provided for these samples to be included in our analysis (García-

541 Comas *et al.*, 2014).

542   While none of the previous studies have examined the vertical structure of

543   continental shelf zooplankton communities in the same detail as horizontal structure,

544   several studies have made similar conclusions to that observed in the current study. In the

545   southeast Atlantic, a higher biomass of zooplankton was found above the pycnocline

546   attributed to the increased chlorophyll-a in these waters (Marcolin *et al.*, 2013). In the

547   northwest Atlantic, a similar strong association was found with a thermocline, with distinct

548   zooplankton communities across the continental shelf separated by the 15° C thermocline

549   (Turner and Dagg, 1983). Similar patterns in zooplankton size structure are observed around

550   thermoclines in subtropical Australia (Suthers *et al.*, 2006).

551

552   *Implications for the future*

553   While the distributions and patterns observed in the current study align with global

554   observations, they are only a snapshot and at other times of the year the patterns may vary.

555   Our analysis of seasonal influence by the EAC showed that while there are seasonal

556   variations in alongshore current velocity due to the EAC (Figure 6), the velocities observed in

557   our study reflect a large portion of the year in terms of the velocities at our transect

558   locations. Despite this, the EAC is strengthening and the increasing water temperatures in

559   the southeast Australian region are already impacting the zooplankton communities as the

560   region becomes increasingly tropicalised (Kelly *et al.*, 2016). At long term observing stations

561   in the southeast Australian region, warming waters have resulted in a reduction in the

562   spring phytoplankton bloom and > 60% decline phytoplankton growth during spring

563   (Thompson *et al.*, 2009). These changes may have significant bottom-up effects on the

564   overall distribution of zooplankton biomass, size structure and community composition on

565 continental shelves as zooplankton are impacted across the globe in similar ways

566 (Richardson, 2008).

567

Conclusions

569   Based upon the previous research into zooplankton distributions on continental

570 shelves and the current study, we suggest a general process for the distribution of

571 zooplankton on continental shelves influenced by boundary currents. This heuristic model

572 includes expectations for future studies to examine, such as the decline in zooplankton

573 biomass with distance offshore and with depth in the water column. This is potentially

574 driven by western boundary currents which drive productivity on the shelf through uplift of

575 nutrient rich waters. Future studies could answer these questions with more sustained

576 monitoring of cross-shelf patterns throughout the year.

577

587

588 **Author Contributions**

589 MEB & IMS conceived the study and collected the data. HTS, JDE, AS & PY analysed the data.

590 HTS wrote the first draft and all authors contributed to and approved the final manuscript.

591

592 **Data Availability**

593 All data used in this study are freely accessible. The data from the Southern Surveyor voyage

594 08/2004 is available from the CSIRO Data Trawler

595 (https://www.marine.csiro.au/data/trawler/). The long term environmental data is available

596 from the Australian Ocean Data Network (https://portal.aodn.org.au/). All code used for the

597 analysis in this paper is available in the GitHub repository

598 https://github.com/HaydenSchilling/Inner-Shelf-Water.

599

600 **Competing Interests Statement**

601 The authors declare no competing interests.

References

Aarflot, J. M., Aksnes, D. L., Opdal, A. F., Skjoldal, H. R., and Fiksen, O. 2019. Caught in broad daylight: Topographic constraints of zooplankton depth distributions. Limnology and Oceanography, 64: 849–859.

Aguiar, A. L., Cirano, M., Pereira, J., and Marta-Almeida, M. 2014. Upwelling processes along a western boundary current in the Abrolhos–Campos region of Brazil. Continental Shelf Research, 85: 42–59.

Akima, H., and Gebhardt, A. 2020. akima: Interpolation of Irregularly and Regularly Spaced Data. R package version 0.6-2.1. https://CRAN.R-project.org/package=akima.

Alldredge, A. L., and Silver, M. W. 1988. Characteristics, dynamics and significance of marine snow. Progress in Oceanography, 20: 41–82.

Andersen, K. H., Berge, T., Gonçalves, R. J., Hartvig, M., Heuschele, J., Hylander, S., Jacobsen, N. S., *et al.* 2016. Characteristic Sizes of Life in the Oceans, from Bacteria to Whales. Annual Review of Marine Science, 8: 217–241.

Apte, S. C., Batley, G. E., Szymczak, R., Rendell, P. S., Lee, R., and Waite, T. D. 1998. Baseline trace metal concentrations in New South Wales coastal waters. Marine and Freshwater Research, 49: 203–214.

Archer, M. R., Roughan, M., Keating, S. R., and Schaeffer, A. 2017. On the Variability of the East Australian Current: Jet Structure, Meandering, and Influence on Shelf Circulation. Journal of Geophysical Research: Oceans, 122: 8464–8481.

Armbrecht, L. H., Roughan, M., Rossi, V., Schaeffer, A., Davies, P. L., Waite, A. M., and Armand, L. K. 2014. Phytoplankton composition under contrasting oceanographic conditions: Upwelling and downwelling (Eastern Australia). Continental Shelf Research, 75: 54–67.

Armbrecht, L. H., Thompson, P. A., Wright, S. W., Schaeffer, A., Roughan, M., Henderiks, J., and Armand, L. K. 2015. Comparison of the cross-shelf phytoplankton distribution of two oceanographically distinct regions off Australia. Journal of Marine Systems, 148: 26–38.

Atkinson, A., Lilley, M. K. S., Hirst, A. G., McEvoy, A. J., Tarran, G. A., Widdicombe, C., Fileman, E. S., *et al.* 2020. Increasing nutrient stress reduces the efficiency of energy transfer through planktonic size spectra. Limnology and Oceanography, n/a. https://aslopubs.onlinelibrary.wiley.com/doi/abs/10.1002/lno.11613 (Accessed 26 October 2020).

Baird, M. E., Timko, P. G., Middleton, J. H., Mullaney, T. J., Cox, D. R., and Suthers, I. M. 2008. Biological properties across the Tasman Front off southeast Australia. Deep-Sea Research Part I-Oceanographic Research Papers, 55: 1438–1455.

Barnes, C., Maxwell, D., Reuman, D. C., and Jennings, S. 2010. Global patterns in predator–prey size relationships reveal size dependency of trophic transfer efficiency. Ecology, 91: 222–232.

Blanchard, J. L., Heneghan, R. F., Everett, J. D., Trebilco, R., and Richardson, A. J. 2017. From Bacteria to Whales: Using Functional Size Spectra to Model Marine Ecosystems. Trends in Ecology & Evolution, 32: 174–186.

Brink, K. H. 2016. Cross-Shelf Exchange. Annual Review of Marine Science, 8: 59–78.

Carr, M.-E., and Kearns, E. J. 2003. Production regimes in four Eastern Boundary Current systems. Deep Sea Research Part II: Topical Studies in Oceanography, 50: 3199–3221.

Cetina-Heredia, P., Roughan, M., van Sebille, E., and Coleman, M. A. 2014. Long-term trends in the East Australian Current separation latitude and eddy driven transport. Journal of Geophysical Research: Oceans, 119: 4351–4366.

35

651 Dai, A., and Trenberth, K. E. 2002. Estimates of Freshwater Discharge from Continents:
652   Latitudinal and Seasonal Variations. Journal of Hydrometeorology, 3: 660–687.

653 Edwards, A. M., Robinson, J. P. W., Plank, M. J., Baum, J. K., and Blanchard, J. L. 2017.
654   Testing and recommending methods for fitting size spectra to data. Methods in
655   Ecology and Evolution, 8: 57–67.

656 Espinasse, B., Basedow, S., Schultes, S., Zhou, M., Berline, L., and Carlotti, F. 2018.
657   Conditions for assessing zooplankton abundance with LOPC in coastal waters.
658   Progress in Oceanography, 163: 260–270.

659 Everett, J. D., Baird, M. E., Oke, P. R., and Suthers, I. M. 2012. An avenue of eddies:
660   Quantifying the biophysical properties of mesoscale eddies in the Tasman Sea.
661   Geophysical Research Letters, 39: 5.

662 Everett, J. D., Baird, M. E., Roughan, M., Suthers, I. M., and Doblin, M. A. 2014. Relative
663   impact of seasonal and oceanographic drivers on surface chlorophyll a along a
664   Western Boundary Current. Progress in Oceanography, 120: 340–351.

665 Fiedler, P. C., and Bernard, H. J. 1987. Tuna aggregation and feeding near fronts observed in
666   satellite imagery. Continental Shelf Research, 7: 871–881.

667 García-Comas, C., Chang, C.-Y., Ye, L., Sastri, A. R., Lee, Y.-C., Gong, G.-C., and Hsieh, C.
668   2014. Mesozooplankton size structure in response to environmental conditions in the
669   East China Sea: How much does size spectra theory fit empirical data of a dynamic
670   coastal area? Progress in Oceanography, 121: 141–157.

671 GEBCO Bathymetric Compilation Group. 2019. The GEBCO_2019 Grid - a continuous
672   terrain model of the global oceans and land.

673 Guiet, J., Poggiale, J.-C., and Maury, O. 2016. Modelling the community size-spectrum:
674   recent developments and new directions. Ecological Modelling, 337: 4–14.

675 Heneghan, R. F., Hatton, I. A., and Galbraith, E. D. 2019. Climate change impacts on marine
676   ecosystems through the lens of the size spectrum. Emerging Topics in Life Sciences,
677   3: 233–243.

678 Herman, A. W. 1992. Design and calibration of a new optical plankton counter capable of
679   sizing small zooplankton. Deep Sea Research Part A. Oceanographic Research
680   Papers, 39: 395–415.

681 Hobday, A. J., and Hartmann, K. 2006. Near real-time spatial management based on habitat
682   predictions for a longline bycatch species. Fisheries Management and Ecology, 13:
683   365–380.

684 Holland, M. M., Smith, J. A., Everett, J. D., Vergés, A., and Suthers, I. M. 2020. Latitudinal
685   patterns in trophic structure of temperate reef-associated fishes and predicted
686   consequences of climate change. Fish and Fisheries, n/a.
687   https://onlinelibrary.wiley.com/doi/abs/10.1111/faf.12488.

688 Irigoien, X., Fernandes, J. A., Grosjean, P., Denis, K., Albaina, A., and Santos, M. 2009.
689   Spring zooplankton distribution in the Bay of Biscay from 1998 to 2006 in relation
690   with anchovy recruitment. Journal of Plankton Research, 31: 1–17.

691 Kelly, P., Clementson, L., Davies, C., Corney, S., and Swadling, K. 2016. Zooplankton
692   responses to increasing sea surface temperatures in the southeastern Australia global
693   marine hotspot. Estuarine, Coastal and Shelf Science, 180: 242–257.

694 Kerr, S. R., and Dickie, L. M. 2001. The biomass spectrum: a predator-prey theory of aquatic
695   production. Columbia University Press.

696 Krupica, K. L., Sprules, W. G., and Herman, A. W. 2012. The utility of body size indices
697   derived from optical plankton counter data for the characterization of marine
698   zooplankton assemblages. Continental Shelf Research, 36: 29–40.

699 Lucas, A. J., Dupont, C. L., Tai, V., Largier, J. L., Palenik, B., and Franks, P. J. S. 2011. The
700   green ribbon: Multiscale physical control of phytoplankton productivity and

community structure over a narrow continental shelf. Limnology and Oceanography, 56: 611–626.

Maia, H. A., Morais, R. A., Quimbayo, J. P., Dias, M. S., Sampaio, C. L. S., Horta, P. A., Ferreira, C. E. L., *et al.* 2018. Spatial patterns and drivers of fish and benthic reef communities at São Tomé Island, Tropical Eastern Atlantic. Marine Ecology, 39: e12520.

Malan, N., Archer, M., Roughan, M., Cetina-Heredia, P., Hemming, M., Rocha, C., Schaeffer, A., *et al.* 2020. Eddy-Driven Cross-Shelf Transport in the East Australian Current Separation Zone. Journal of Geophysical Research: Oceans, 125: e2019JC015613.

Marcolin, C. da R., Schultes, S., Jackson, G. A., and Lopes, R. M. 2013. Plankton and seston size spectra estimated by the LOPC and ZooScan in the Abrolhos Bank ecosystem (SE Atlantic). Continental Shelf Research, 70: 74–87.

Marcolin, C. da R., Lopes, R. M., and Jackson, G. A. 2015. Estimating zooplankton vertical distribution from combined LOPC and ZooScan observations on the Brazilian Coast. Marine Biology, 162: 2171–2186.

Moore, S. K., and Suthers, I. M. 2006. Evaluation and correction of subresolved particles by the optical plankton counter in three Australian estuaries with pristine to highly modified catchments. Journal of Geophysical Research: Oceans, 111.

Nakata, H., Kimura, S., Okazaki, Y., and Kasai, A. 2000. Implications of meso-scale eddies caused by frontal disturbances of the Kuroshio Current for anchovy recruitment. ICES Journal of Marine Science, 57: 143–152.

Nogueira, E., González-Nuevo, G., Bode, A., Varela, M., Morán, X. A. G., and Valdés, L. 2004. Comparison of biomass and size spectra derived from optical plankton counter data and net samples: application to the assessment of mesoplankton distribution along the Northwest and North Iberian Shelf. ICES Journal of Marine Science, 61: 508–517. Oxford Academic.

Oke, P. R., Roughan, M., Cetina-Heredia, P., Pilo, G. S., Ridgway, K. R., Rykova, T., Archer, M. R., *et al.* 2019. Revisiting the circulation of the East Australian Current: Its path, separation, and eddy field. Progress in Oceanography, 176: 102139.

Pauly, D., Christensen, V., Guénette, S., Pitcher, T. J., Sumaila, U. R., Walters, C. J., Watson, R., *et al.* 2002. Towards sustainability in world fisheries. Nature, 418: 689–695. Nature Publishing Group.

Pereira Brandini, F., Nogueira, M., Simião, M., Carlos Ugaz Codina, J., and Almeida Noernberg, M. 2014. Deep chlorophyll maximum and plankton community response to oceanic bottom intrusions on the continental shelf in the South Brazilian Bight. Continental Shelf Research, 89: 61–75.

Pritchard, T. R., Lee, R. S., Ajani, P. A., Rendell, P. S., Black, K., and Koop, K. 2003. Phytoplankton Responses to Nutrient Sources in Coastal Waters off Southeastern Australia. Aquatic Ecosystem Health & Management, 6: 105–117. Taylor & Francis.

Reese, D. C., O'Malley, R. T., Brodeur, R. D., and Churnside, J. H. 2011. Epipelagic fish distributions in relation to thermal fronts in a coastal upwelling system using high-resolution remote-sensing techniques. ICES Journal of Marine Science, 68: 1865–1874. Oxford Academic.

Revill, A. T., Young, J. W., and Lansdell, M. 2009. Stable isotopic evidence for trophic groupings and bio-regionalization of predators and their prey in oceanic waters off eastern Australia. Marine Biology, 156: 1241–1253.

Richardson, A. J. 2008. In hot water: zooplankton and climate change. ICES Journal of Marine Science, 65: 279–295.

750 Ridgway, K. R., and Dunn, J. R. 2003. Mesoscale structure of the mean East Australian
751 Current System and its relationship with topography. Progress in Oceanography, 56:
752 189–222.
753 Rossi, V., Schaeffer, A., Wood, J., Galibert, G., Morris, B., Sudre, J., Roughan, M., *et al.*
754 2014. Seasonality of sporadic physical processes driving temperature and nutrient
755 high-frequency variability in the coastal ocean off southeast Australia. Journal of
756 Geophysical Research: Oceans, 119: 445–460.
757 Roughan, M., and Middleton, J. H. 2002. A comparison of observed upwelling mechanisms
758 off the east coast of Australia. Continental Shelf Research, 22: 2551–2572.
759 Sabatès, A., Gili, J. M., and Pagès, F. 1989. Relationship between zooplankton distribution,
760 geographic characteristics and hydrographic patterns off the Catalan coast (Western
761 Mediterranean). Marine Biology, 103: 153–159.
762 Schaeffer, A., Roughan, M., and Morris, B. D. 2013. Cross-shelf dynamics in a western
763 boundary current regime: Implications for upwelling. Journal of Physical
764 Oceanography, 44: 2812–2813.
765 Schaeffer, A., Roughan, M., and Wood, J. E. 2014. Observed bottom boundary layer
766 transport and uplift on the continental shelf adjacent to a western boundary current.
767 Journal of Geophysical Research-Oceans, 119: 4922–4939.
768 Schaeffer, A., and Roughan, M. 2015. Influence of a western boundary current on shelf
769 dynamics and upwelling from repeat glider deployments. Geophysical Research
770 Letters, 42: 121–128.
771 Sourisseau, M., and Carlotti, F. 2006. Spatial distribution of zooplankton size spectra on the
772 French continental shelf of the Bay of Biscay during spring 2000 and 2001. Journal of
773 Geophysical Research: Oceans, 111.
774 Sprules, W. G., and Barth, L. E. 2015. Surfing the biomass size spectrum: some remarks on
775 history, theory, and application. Canadian Journal of Fisheries and Aquatic Sciences,
776 73: 477–495. NRC Research Press.
777 Suthers, I. M., Taggart, C. T., Rissik, D., and Baird, M. E. 2006. Day and night
778 ichthyoplankton assemblages and zooplankton biomass size spectrum in a deep ocean
779 island wake. Marine Ecology Progress Series, 322: 225–238.
780 Suthers, I. M., Everett, J. D., Roughan, M., Young, J. W., Oke, P. R., Condie, S. A., Hartog,
781 J. R., *et al.* 2011. The strengthening East Australian Current, its eddies and biological
782 effects - an introduction and overview. Deep-Sea Research Part II-Topical Studies in
783 Oceanography, 58: 538–546.
784 Thompson, P. A., Baird, M. E., Ingleton, T., and Doblin, M. A. 2009. Long-term changes in
785 temperate Australian coastal waters: implications for phytoplankton. Marine Ecology
786 Progress Series, 394: 1–19.
787 Truong, L., Suthers, I. M., Cruz, D. O., and Smith, J. A. 2017. Plankton supports the majority
788 of fish biomass on temperate rocky reefs. Marine Biology, 164: 12.
789 Tsukamoto, K., and Miller, M. J. 2020. The mysterious feeding ecology of leptocephali: a
790 unique strategy of consuming marine snow materials. Fisheries Science.
791 https://doi.org/10.1007/s12562-020-01477-3 (Accessed 14 December 2020).
792 Turner, J. T., and Dagg, M. J. 1983. Vertical Distributions of Continental Shelf Zooplankton
793 in Stratified and Isothermal Waters. Biological Oceanography, 3: 1–40.
794 Vandromme, P., Nogueira, E., Huret, M., Lopez-Urrutia, Á., González, G. G.-N., Sourisseau,
795 M., and Petitgas, P. 2014. Springtime zooplankton size structure over the continental
796 shelf of the Bay of Biscay. Ocean Science, 10: 821–835.
797 Vidondo, B., Prairie, Y. T., Blanco, J. M., and Duarte, C. M. 1997. Some aspects of the
798 analysis of size spectra in aquatic ecology. Limnology and Oceanography, 42: 184–
799 192.

800 Wallis, J. R., Swadling, K. M., Everett, J. D., Suthers, I. M., Jones, H. J., Buchanan, P. J.,
801   Crawford, C. M., *et al.* 2016. Zooplankton abundance and biomass size spectra in the
802   East Antarctic sea-ice zone during the winter–spring transition. Deep Sea Research
803   Part II: Topical Studies in Oceanography, 131: 170–181.
804 White, E. P., Ernest, S. K. M., Kerkhoff, A. J., and Enquist, B. J. 2007. Relationships
805   between body size and abundance in ecology. Trends in Ecology & Evolution, 22:
806   323–330.
807 Wickham, H. 2011. ggplot2. WIREs Computational Statistics, 3: 180–185.
808 Wood, J. E., Schaeffer, A., Roughan, M., and Tate, P. M. 2016. Seasonal variability in the
809   continental shelf waters off southeastern Australia: Fact or fiction? Continental Shelf
810   Research, 112: 92–103.
811

Click here to access/download

e-Component

Schilling et al Supplementary_8_1_20.docx